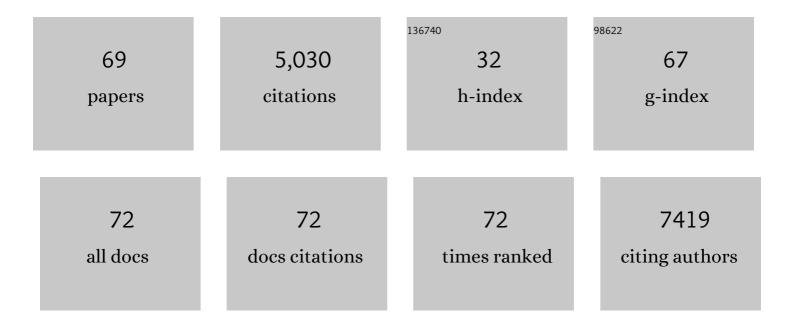
Christopher Allen

List of Publications by Year in descending order

Source: https://exaly.com/author-pdf/5436368/publications.pdf Version: 2024-02-01



#	Article	IF	CITATIONS
1	Lowâ€Coordinated CoNC on Oxygenated Graphene for Efficient Electrocatalytic H ₂ O ₂ Production. Advanced Functional Materials, 2022, 32, 2106886.	7.8	97
2	Aberration-corrected transmission electron microscopy of a non-graphitizing carbon. Proceedings of the Royal Society A: Mathematical, Physical and Engineering Sciences, 2022, 478, .	1.0	4
3	Counting molecules in nano test tubes: a method for determining the activation parameters of thermally driven reactions through direct imaging. Chemical Communications, 2021, 57, 10628-10631.	2.2	1
4	Single-molecule imaging and kinetic analysis of intermolecular polyoxometalate reactions. Chemical Science, 2021, 12, 7377-7387.	3.7	18
5	Sulfur Promotion in Au/C Catalyzed Acetylene Hydrochlorination. Small, 2021, 17, 2007221.	5.2	16
6	Atomic resolution HOLZ-STEM imaging of atom position modulation in oxide heterostructures. Ultramicroscopy, 2021, 226, 113296.	0.8	4
7	Quantifying the performance of a hybrid pixel detector with GaAs:Cr sensor for transmission electron microscopy. Ultramicroscopy, 2021, 227, 113298.	0.8	12
8	Mechanistic insight into the active centers of single/dual-atom Ni/Fe-based oxygen electrocatalysts. Nature Communications, 2021, 12, 5589.	5.8	173
9	Edge-hosted Fe-N3 sites on a multiscale porous carbon framework combining high intrinsic activity with efficient mass transport for oxygen reduction. Chem Catalysis, 2021, 1, 1291-1307.	2.9	86
10	Bifunctional Single Atom Electrocatalysts: Coordination–Performance Correlations and Reaction Pathways. ACS Nano, 2020, 14, 13279-13293.	7.3	107
11	Transforming Transmission Electron Microscopy with MerlinEM Electron Counting Detector. Microscopy and Microanalysis, 2020, 26, 1944-1945.	0.2	1
12	Adsorption and activation of molecular oxygen over atomic copper(I/II) site on ceria. Nature Communications, 2020, 11, 4008.	5.8	95
13	A fundamental look at electrocatalytic sulfur reduction reaction. Nature Catalysis, 2020, 3, 762-770.	16.1	455
14	Phase Variations and Layer Epitaxy of 2D PdSe ₂ Grown on 2D Monolayers by Direct Selenization of Molecular Pd Precursors. ACS Nano, 2020, 14, 11677-11690.	7.3	10
15	Focused-probe STEM Ptychography: Developments and Opportunities. Microscopy and Microanalysis, 2020, 26, 470-471.	0.2	0
16	Detectors—The ongoing revolution in scanning transmission electron microscopy and why this important to material characterization. APL Materials, 2020, 8, .	2.2	44
17	Low-dose phase retrieval of biological specimens using cryo-electron ptychography. Nature Communications, 2020, 11, 2773.	5.8	72
18	Phase reconstruction using fast binary 4D STEM data. Applied Physics Letters, 2020, 116, .	1.5	34

CHRISTOPHER ALLEN

#	Article	IF	CITATIONS
19	Automated Single-Particle Reconstruction of Heterogeneous Inorganic Nanoparticles. Microscopy and Microanalysis, 2020, 26, 1168-1175.	0.2	13
20	Effects of Rashba-spin–orbit coupling on superconducting boron-doped nanocrystalline diamond films: evidence of interfacial triplet superconductivity. New Journal of Physics, 2020, 22, 093039.	1.2	6
21	Simultaneous Identification of Low and High Atomic Number Atoms in Monolayer 2D Materials Using 4D Scanning Transmission Electron Microscopy. Nano Letters, 2019, 19, 6482-6491.	4.5	36
22	Electron Ptychography Using Fast Binary 4D STEM Data. Microscopy and Microanalysis, 2019, 25, 1662-1663.	0.2	3
23	Electron ptychography using an ultrafast direct electron detector. Microscopy and Microanalysis, 2019, 25, 20-21.	0.2	1
24	Observing Structural Dynamics and Measuring Chemical Kinetics in Low Dimensional Materials Using High Speed Imaging. Microscopy and Microanalysis, 2019, 25, 1682-1683.	0.2	2
25	Low-Dose Scanning Electron Diffraction Microscopy of Mechanochemically Nanostructured Pharmaceuticals. Microscopy and Microanalysis, 2019, 25, 1746-1747.	0.2	6
26	In situ high temperature atomic level dynamics of large inversion domain formations in monolayer MoS2. Nanoscale, 2019, 11, 1901-1913.	2.8	19
27	Atomic electrostatic maps of 1D channels in 2D semiconductors using 4D scanning transmission electron microscopy. Nature Communications, 2019, 10, 1127.	5.8	62
28	Atomic Resolution Defocused Electron Ptychography at Low Dose with a Fast, Direct Electron Detector. Scientific Reports, 2019, 9, 3919.	1.6	44
29	Formation and Healing of Defects in Atomically Thin GaSe and InSe. ACS Nano, 2019, 13, 5112-5123.	7.3	35
30	Molecular nitrogen promotes catalytic hydrodeoxygenation. Nature Catalysis, 2019, 2, 1078-1087.	16.1	63
31	Imaging the atomic structure and local chemistry of platelets in natural type Ia diamond. Nature Materials, 2018, 17, 243-248.	13.3	17
32	General synthesis and definitive structural identification of MN4C4 single-atom catalysts with tunable electrocatalytic activities. Nature Catalysis, 2018, 1, 63-72.	16.1	1,476
33	A quantitative method for measuring small residual beam tilts in high-resolution transmission electron microscopy. Ultramicroscopy, 2018, 184, 18-28.	0.8	1
34	Hollow Electron Ptychographic Diffractive Imaging. Physical Review Letters, 2018, 121, 146101.	2.9	27
35	Low Dose Defocused Probe Electron Ptychography Using a Fast Direct Electron Detector. Microscopy and Microanalysis, 2018, 24, 186-187.	0.2	5
36	Fast and Low-dose Electron Ptychography. Microscopy and Microanalysis, 2018, 24, 224-225.	0.2	3

CHRISTOPHER ALLEN

#	Article	IF	CITATIONS
37	Ultralong 1D Vacancy Channels for Rapid Atomic Migration during 2D Void Formation in Monolayer MoS ₂ . ACS Nano, 2018, 12, 7721-7730.	7.3	54
38	Imaging Structure and Magnetisation in New Ways Using 4D STEM. Microscopy and Microanalysis, 2018, 24, 180-181.	0.2	1
39	Low-dose scanning electron diffraction and pharmaceutical nanostructure. Acta Crystallographica Section A: Foundations and Advances, 2018, 74, e83-e84.	0.0	0
40	Atomic Structure and Dynamics of Single Platinum Atom Interactions with Monolayer MoS ₂ . ACS Nano, 2017, 11, 3392-3403.	7.3	126
41	Atomic structure and formation mechanism of sub-nanometer pores in 2D monolayer MoS ₂ . Nanoscale, 2017, 9, 6417-6426.	2.8	54
42	Orientation dependent interlayer stacking structure in bilayer MoS ₂ domains. Nanoscale, 2017, 9, 13060-13068.	2.8	19
43	Atomically Flat Zigzag Edges in Monolayer MoS ₂ by Thermal Annealing. Nano Letters, 2017, 17, 5502-5507.	4.5	70
44	<i>In Situ</i> Atomic-Scale Studies of the Formation of Epitaxial Pt Nanocrystals on Monolayer Molybdenum Disulfide. ACS Nano, 2017, 11, 9057-9067.	7.3	27
45	Aberration measurement of the probe-forming system of an electron microscope using two-dimensional materials. Ultramicroscopy, 2017, 182, 195-204.	0.8	5
46	Characterization of thin film displacements in the electron microscope. Applied Physics Letters, 2017, 111, 203104.	1.5	0
47	Response to "Comment on †Temperature dependence of atomic vibrations in mono-layer graphene'―[Appl. Phys. 119, 066101 (2016)]. Journal of Applied Physics, 2016, 119, 066102.	l. _{1.1}	1
48	One-Pot Synthesis of Lithium-Rich Cathode Material with Hierarchical Morphology. Nano Letters, 2016, 16, 7503-7508.	4.5	42
49	Atomic Structure and Spectroscopy of Single Metal (Cr, V) Substitutional Dopants in Monolayer MoS ₂ . ACS Nano, 2016, 10, 10227-10236.	7.3	96
50	Electron Exit Wave Reconstruction From a Single Defocused Image Using a Gaussian Basis. Microscopy and Microanalysis, 2015, 21, 745-746.	0.2	1
51	Temperature dependence of atomic vibrations in mono-layer graphene. Journal of Applied Physics, 2015, 118, .	1.1	18
52	Controlled formation of closed-edge nanopores in graphene. Nanoscale, 2015, 7, 11602-11610.	2.8	38
53	Temperature Dependence of the Reconstruction of Zigzag Edges in Graphene. ACS Nano, 2015, 9, 4786-4795.	7.3	68
54	Thermally Induced Dynamics of Dislocations in Graphene at Atomic Resolution. ACS Nano, 2015, 9, 10066-10075.	7.3	36

CHRISTOPHER ALLEN

#	Article	IF	CITATIONS
55	Partial Dislocations in Graphene and Their Atomic Level Migration Dynamics. Nano Letters, 2015, 15, 5950-5955.	4.5	37
56	Optically enhanced charge transfer between C ₆₀ and single-wall carbon nanotubes in hybrid electronic devices. Nanoscale, 2014, 6, 572-580.	2.8	9
57	Dynamics of Single Fe Atoms in Graphene Vacancies. Nano Letters, 2013, 13, 1468-1475.	4.5	228
58	Structural Reconstruction of the Graphene Monovacancy. ACS Nano, 2013, 7, 4495-4502.	7.3	131
59	Visible light-driven CO ₂ reduction by enzyme coupled CdS nanocrystals. Chemical Communications, 2012, 48, 58-60.	2.2	184
60	Spatial control of defect creation in graphene at the nanoscale. Nature Communications, 2012, 3, 1144.	5.8	305
61	The Identification of Inner Tube Defects in Doubleâ€Wall Carbon Nanotubes. Small, 2012, 8, 3810-3815.	5.2	5
62	Large Single Crystals of Graphene on Melted Copper Using Chemical Vapor Deposition. ACS Nano, 2012, 6, 5010-5017.	7.3	218
63	Two-Dimensional Coalescence Dynamics of Encapsulated Metallofullerenes in Carbon Nanotubes. ACS Nano, 2011, 5, 10084-10089.	7.3	31
64	Transport measurements on carbon nanotubes structurally characterized by electron diffraction. Physical Review B, 2011, 84, .	1.1	4
65	A review of methods for the accurate determination of the chiral indices of carbon nanotubes from electron diffraction patterns. Carbon, 2011, 49, 4961-4971.	5.4	34
66	Device fabrication with precisely placed carbon nanotubes of known chiral vector. Journal of Physics: Conference Series, 2010, 241, 012082.	0.3	4
67	Growth of vertically-aligned carbon nanotube forests on conductive cobalt disilicide support. Journal of Applied Physics, 2010, 108, .	1.1	53
68	Magnetic field enhanced nano-tip fabrication for four-probe STM studies. Nanotechnology, 2008, 19, 085201.	1.3	11
69	Four-probe electrical transport measurements on individual metallic nanowires. Nanotechnology, 2007, 18, 065204.	1.3	71